Optimal Single Resistor Damping of Input Filters

Robert W. Erickson
Colorado Power Electronics Center
University of Colorado
Boulder, Colorado 80309-0425
rwe@boulder.colorado.edu

ABSTRACT—A general procedure is outlined for optimizing the damping of an input filter using a single resistor. This procedure is employed to derive the equations governing optimal damping of several basic filter circuits. Design tradeoffs are discussed. Additional criteria are derived that allow employment of these results in design of multiple-section cascaded filters with damping.

I. INTRODUCTION

The need for damping in the *L-C* input filters of switching converters is well appreciated within the power electronics field [1-7]. Adequate filter damping may be necessary to avoid destabilizing the feedback loops of dc-dc converters with duty cycle control [1,2] or current-programmed control [4,5]. In aerospace applications, damping is needed to avoid excessive capacitor currents during conducted susceptibility tests. Some low-harmonic rectifier approaches also require an input filter; in these cases, filter damping may also be required to avoid degradation of the converter control system.

Damping of an input filter can significantly increase its size and cost. Hence, approaches for efficient design of damped input filters have been suggested [2,3,7]. In this paper, the optimal damping approach of [2] is extended to two other filter topologies, and application of the results to multiple-section cascaded filters is illustrated.

A. Review of Input Filter Design Criteria

Whenever feedback is applied to regulate the output of a high-efficiency converter, the converter presents a constant-power load to its input port [8]. The incremental resistance of a constant-power load characteristic is negative; connection of this negative incremental resistance to an L-C input filter can lead to oscillation when the filter is insufficiently damped [6].

The dynamics of the converter and its control system further complicate the input filter stability problem. A complete set of input filter design criteria that account for dynamics of duty-ratio-controlled converters was derived in [1]. This paper made use of Middlebrook's extra element theorem [8] to show how addition of an input filter modifies the converter loop gain and other important quantities. For example, the modified loop gain was shown to be:

$$T'(s) = T(s)\left(1 + \frac{Z_o(s)}{Z_{iN}(s)}\right) \Big/\!\!/ \left(1 + \frac{Z_o(s)}{Z_{iD}(s)}\right) \tag{1}$$

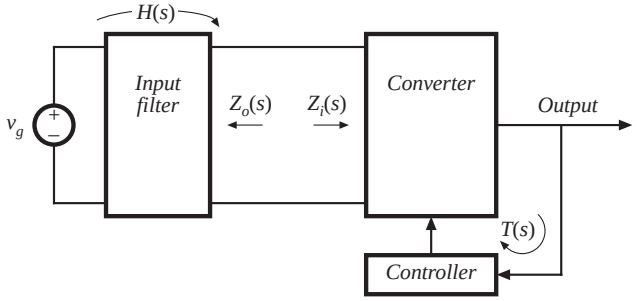

Fig. 1 Addition of an input filter to a converter system.

where $T(s)$ is the original loop gain (with no input filter), $T'(s)$ is the modified loop gain (in the presence of the input filter), and $Z_o(s)$ is the filter output impedance. $Z_{iN}(s)$ is the converter input impedance $Z_i(s)$ under the condition that the controller operates ideally; for conventional duty cycle control, $Z_{iN}(s)$ is equal to the negative incremental input resistance $-R/M^2$ where R is the load resistance and M is the conversion ratio of the converter. $Z_{iD}(s)$ is the open-loop input impedance of the converter.

It can be seen from Eq. 1 that addition of the input filter does not significantly modify the converter loop gain provided that

$$\begin{aligned} \| Z_o \| &<< \| Z_{iN} \|, \text{ and} \\ \| Z_o \| &<< \| Z_{iD} \| \end{aligned} \tag{2}$$

These inequalities limit the maximum allowable output impedance of the input filter, and constitute useful filter design criteria.

Equations (1) and (2) explain why undamped *L-C* input filters (such as Fig. 2) lead to converter oscillation. The output impedance $Z_o(s)$ tends to infinity at the filter resonant frequency f_0:

$$f_0 = \frac{1}{2\pi\sqrt{LC}} \tag{3}$$

Impedance inequalities (2) are therefore violated near $f = f_0$, and possibly at other frequencies as well. For this case, it can be shown that the modified loop gain $T'(s)$ of Eq. (1) contains

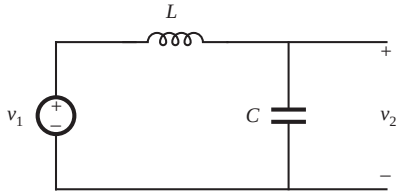

Fig. 2 Basic undamped single-section input filter.

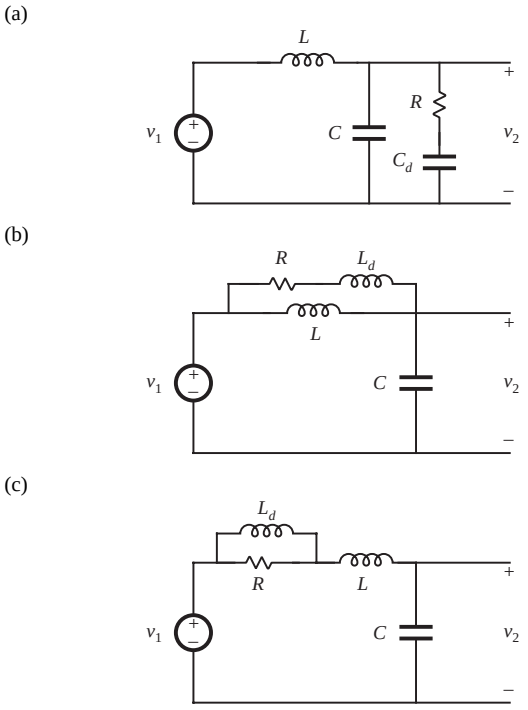

Fig. 3 Three approaches to damping the single-section input filter: (a) shunt R-C_d damping network, (b) parallel damping resistor R with high-frequency series blocking inductor, (c) series damping resistor with parallel dc bypass inductor.

a complex pole pair and a complex right-half-plane (nonminimum phase) zero pair in the vicinity of the filter resonant frequency f_0. This introduces an additional 360° of phase lag into the converter loop gain $T'(s)$ at frequencies greater than f_0. If the feedback loop crossover frequency is greater than f_0, then negative phase margin and instability are very difficult to avoid.

Similar impedance inequalities have been derived for the case of current-programmed converters [4,5]. Filter impedance inequalities were expressed in terms of converter y-parameters in [5]. In [4], impedance inequalities nearly identical to the duty-ratio-controlled case (Eq. (2)) were derived.

Feedforward of the converter input voltage was suggested in [7]. This approach allows reduction of damping element size, provided that the input filter contains a sufficient minimal amount of damping.

B. The Filter Damping Problem

A basic undamped L-C single-section filter is illustrated in Fig. 2, and several approaches for damping its resonance are shown in Fig. 3. Figure 3(a) illustrates the addition of a shunt R-C_d damping network; this approach was used in [1]. Modification of an input filter to reduce its peak output impedance invariably involves increased capacitance values; unless properly designed, the dc blocking capacitor C_d of the R-C_d damping scheme can become large and expensive. Reference [2] described how to optimize the choice of R and C_d; this approach can significantly reduce the size of the damping capacitor. Here, "optimal" refers to the choice of C_d that leads to the minimum peak output impedance, for a given value of R. The problem can also be formulated in an alternate but equivalent form: the choice of R that leads to the minimum peak output impedance, for a given choice of C_d. Damping the filter of Fig. 3(a) to optimize filter input impedance or the filter transfer function was also considered in [2].

Several other damped input filters were discussed in [3], including the use of an R-L_d damping network. Two approaches to single-section filters with R-L_d damping are illustrated in Fig. 3(b) and 3(c). The size of the inductor of the R-L_d damping approach is often much smaller than the added blocking capacitor C_d of the R-C_d damping network. For this reason, R-L_d damping is often the preferred approach in high-density dc-dc converters. When it is necessary to damp the input filter of a low-harmonic rectifier, R-L_d damping is also preferred; this avoids the rectifier peak detection induced by the large blocking capacitor of the R-C_d damping approach.

C. Outline of Discussion

The objective of this paper is to extend the optimization and design procedure of [2] to other basic input filter configurations. Secion II contains a general derivation for optimal design of single-resistor damping networks, based on Middlebrook's extra element theorem [9].

Specific results for the single-section filters of Fig. 3 are listed in Sections III, IV, and V.

An approach to design higher-order filters consisting of cascaded L-C filter sections is contained in Section IV. This approach can lead to a filter of reduced size, consisting of stagger-tuned filter sections. Each L-C section can be one of the optimally-damped networks of Fig. 3. Design charts that quantify the effect of an added filter section on the overall filter output impedance are presented. A two-section design example is included.

II. Filter Optimization

Optimization of an input filter refers here to selection of the damping element such that the peak filter output impedance is minimized.

The dependence of the filter output impedance $Z(s)$ on the damping resistance R can be expressed using Middlebrook's extra element theorem [9] as follows:

$$Z(s) = Z_\infty(s)\frac{\left(1+\frac{Z_N(s)}{R}\right)}{\left(1+\frac{Z_D(s)}{R}\right)} = Z_0(s)\frac{\left(1+\frac{R}{Z_N(s)}\right)}{\left(1+\frac{R}{Z_D(s)}\right)} \tag{4}$$

where $Z_\infty(s)$ and $Z_0(s)$ are the output impedance when R tends to infinity and zero, respectively. $Z_N(s)$ and $Z_D(s)$ are the impedances seen by R when the filter output voltage is nulled and the filter is unloaded, respectively. It can be shown that $Z_\infty(s) = Z_0(s)Z_D(s)/Z_N(s)$. Furthermore, since $Z_\infty(s)$, $Z_0(s)$, $Z_D(s)$,

and $Z_N(s)$ are composed only of inductors and capacitors, $Z_\infty(j\omega)$, $Z_0(j\omega)$, $Z_D(j\omega)$, and $Z_N(j\omega)$ are purely imaginary quantities. Hence, the filter output impedance magnitude can be expressed as [10]:

$$\begin{aligned}\left\| Z(j\omega) \right\|^2 &= Z(j\omega)\overline{Z}(j\omega) \\ &= Z_\infty(j\omega)\frac{\left(1+\frac{Z_N(j\omega)}{R}\right)}{\left(1+\frac{Z_D(j\omega)}{R}\right)}\overline{Z_\infty}(j\omega)\frac{\left(1+\frac{\overline{Z_N}(j\omega)}{R}\right)}{\left(1+\frac{\overline{Z_D}(j\omega)}{R}\right)} \\ &= \left\| Z_\infty(j\omega) \right\|^2 \frac{\left(1+\left\| Z_N(j\omega) \right\|^2/R^2\right)}{\left(1+\left\| Z_D(j\omega) \right\|^2/R^2\right)} \\ &= \left\| Z_0(j\omega) \right\|^2 \frac{\left(1+R^2/\left\| Z_N(j\omega) \right\|^2\right)}{\left(1+R^2/\left\| Z_D(j\omega) \right\|^2\right)}\end{aligned} \tag{5}$$

where $\overline{Z}(j\omega)$ denotes the complex conjugate of $Z(j\omega)$.

At any frequency f_m where $\| Z_N \| = \| Z_D \|$ (which coincides with $\| Z_\infty \| = \| Z_0 \|$), Eq. (5) becomes independent of R. The choice of R does not affect the value of $\| Z \|$ at $f = f_m$, and hence the optimal damping occurs for the choice of R that causes the maximum $\| Z \|$ to occur at $f = f_m$[2]. This fact is used to optimize the filter. $\| Z_\infty \|$ is equated to $\| Z_0 \|$, to find simple expressions for f_m and the optimum peak filter impedance $\| Z(j\omega_m) \|$. The value of R is then found that causes the derivative of $\| Z(j\omega) \|$ to be zero at $\omega = \omega_m$.

III. R-L_d Parallel Damping

Figure 3(b) illustrates the placement of damping resistor R in parallel with inductor L. Inductor L_d causes the filter to exhibit a two-pole attenuation characteristic at high frequency. To allow R to damp the filter, inductor L_d should have an impedance magnitude that is sufficiently smaller that R at the filter resonant frequency.

With this approach, inductor L_d can be physically much smaller than L. Since R is typically much greater than the dc resistance of L, essentially none of the dc output current flows through L_d. Furthermore, R can be realized as the equivalent series resistance of L_d at the filter resonant frequency. Hence, this is a very simple, low-cost approach to damping the input filter.

The disadvantage of this approach is the fact that the high-frequency attenuation of the filter is degraded: the high-frequency asymptote of the filter transfer function is increased from $1/\omega^2 LC$ to $1/\omega^2(L\|L_d)C$. Furthermore, since the need for damping limits the maximum value of L_d, significant loss of high frequency filter attenuation is unavoidable. A tradeoff occurs between damping and degradation of high frequency attenuation, as illustrated in Fig. 4. For example, limiting the degradation of high frequency attenuation to 6 dB leads to an optimum peak filter output impedance of $\sqrt{6}$ times the original characteristic impedance. Additional damping leads to further degradation of the high frequency attenuation. If it is unacceptable that high frequency attenuation be degraded, then the size of inductor L must be increased.

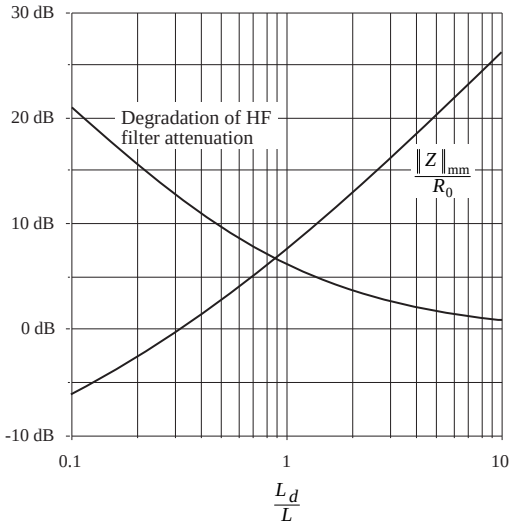

Fig. 4 Performance attained via optimal design procedure, parallel R-L_d circuit of Fig. 3(b). Optimum peak filter output impedance $\| Z \|_{mm}$ and increase of filter high-frequency gain, vs. $n = L_d/L$.

The optimally-damped design (i.e., the choice of R that minimizes the peak output impedance, for a given choice of L_d) is described by the following equations:

$$Q_{opt} = \sqrt{\frac{n(3+4n)(1+2n)}{2(1+4n)}} \tag{6}$$

where

$$n = \frac{L_d}{L} \tag{7}$$

$$Q_{opt} = \frac{optimum\ value\ of\ R}{R_0} \tag{8}$$

$$R_0 = \sqrt{\frac{L}{C}} \tag{9}$$

$$f_0 = \frac{1}{2\pi\sqrt{LC}} \tag{10}$$

The peak filter output impedance occurs at frequency

$$f_m = f_0\sqrt{\frac{1+2n}{2n}} \tag{11}$$

and has value

$$\frac{\| Z \|_{mm}}{R_0} = \sqrt{2n(1+2n)} \tag{12}$$

The attenuation of the filter high-frequency asymptote is degraded by the factor

$$\frac{L}{L\|L_d} = 1 + \frac{1}{n} \tag{13}$$

So given an undamped L-C filter having corner frequency and characteristic impedance given by Eqs. (9) and (10), and given a requirement for the maximum allowable output impedance $\|$

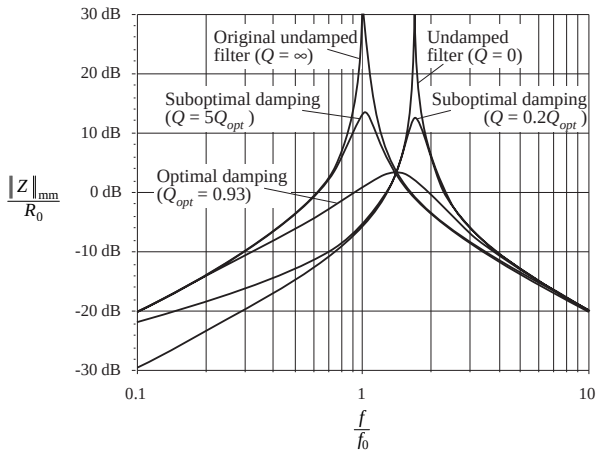

Fig. 5 Comparison of output impedance curves for optimal parallel R-L_d damping with undamped and several suboptimal designs. For this example, $n = L_d/L = 0.516$.

$Z\|_{mm}$, one can solve Eq. (12) for the required value of n. Evaluation of Eq. (6) then leads to the required Q_{opt}. One can then evaluate Eqs. (7) and (8) to find L_d and R.

The optimum filter output impedance magnitude curve obtained via this procedure is compared with undamped and suboptimal curves (having different values of R) in Fig. 5. It can be seen that all curves do indeed pass through a common point corresponding to $f = f_m$, and that the optimal curve peaks at this point.

IV. R-L_d Series Damping

Figure 3(c) illustrates the placement of damping resistor R in series with inductor L. Inductor L_d provides a dc bypass, to avoid significant power dissipation in R. To allow R to damp the filter, inductor L_d should have an impedance magnitude that is sufficiently greater that R at the filter resonant frequency.

Although this circuit is theoretically equivalent to the parallel-damping R-L_d case, several differences are observed in practical design. Both inductors must carry the full dc current, and hence both have significant size. The filter high-frequency attenuation is not affected by the choice of L_d, and the high-frequency asymptote is identical to that of the original undamped filter. The tradeoff in design of this filter does not involve high-frequency attenuation; rather, the issue is damping vs. bypass inductor size.

Design equations similar to those of the previous section can be derived for this case. The optimum peak filter output impedance occurs at frequency

$$f_m = f_0\sqrt{\frac{2+n}{2(1+n)}} \tag{14}$$

and has value

$$\frac{\|Z\|_{mm}}{R_0} = \frac{\sqrt{2(1+n)(2+n)}}{n} \tag{15}$$

The value of damping resistance that leads to optimum damping is described by

$$Q_{opt} = \frac{R_0}{R} = \left(\frac{1+n}{n}\right)\sqrt{\frac{2(1+n)(4+n)}{(2+n)(4+3n)}} \tag{16}$$

The quantities n, f_0, and R_0 are again defined as in Eqs. (7), (9), and (10).

For this case, the peak output impedance cannot be reduced below $\sqrt{2}\,R_0$ via damping. Nonetheless, it is possible to further reduce the filter output impedance by redesign of L and C to reduce R_0.

V. R-C_d Parallel Damping

Figure 3(a) illustrates the placement of damping resistor R in parallel with capacitor C. Capacitor C_d blocks dc current, to avoid significant power dissipation in R. To allow R to damp the filter, capacitor C_d should have an impedance magnitude that is sufficiently less that R at the filter resonant frequency. Optimization of this filter network was described in [2]; results are summarized here for completeness.

The filter high-frequency attenuation is not affected by the choice of C_d, and the high-frequency asymptote is identical to that of the original undamped filter. The tradeoff in design of this filter is damping vs. blocking capacitor size.

For this filter, the quantity n is defined as follows:

$$n = \frac{C_d}{C} \tag{17}$$

The optimum peak filter output impedance occurs at frequency

$$f_m = f_0\sqrt{\frac{2}{2+n}} \tag{18}$$

and has value

$$\frac{\|Z\|_{mm}}{R_0} = \frac{\sqrt{2(2+n)}}{n} \tag{19}$$

The value of damping resistance that leads to optimum damping is described by

$$Q_{opt} = \frac{R}{R_0} = \sqrt{\frac{(2+n)(4+3n)}{2n^2(4+n)}} \tag{20}$$

VI. Cascading Filter Sections

It is well known that a cascade connection of multiple L-C filter sections can achieve a given high-frequency attenuation with less volume and weight than a single-section L-C filter. The increased cutoff frequency of the multiple-section filter allows use of smaller inductance and capacitance values. Damping of each L-C section is usually required, which implies that damping of each section should be optimized. Unfortunately, the optimization method derived in Section II is restricted to filters having only one resistive element. Interactions between cascaded L-C sections can lead to additional resonances and increased filter output impedance.

It is nonetheless possible to design cascaded filter sections such that interaction between sections is negligible. In the approach described below, the filter output impedance

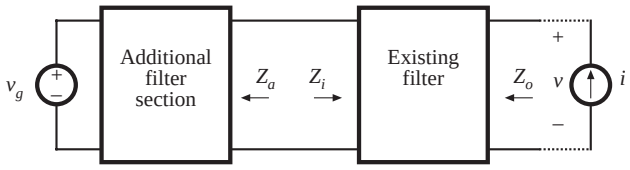

Fig. 6 Addition of a filter section at the input of an existing input filter.

is approximately equal to the output impedance of the last stage, and resonances caused by interactions between stages are avoided. The resulting filter is not "optimal" in any sense; nonetheless, insight can be gained that allows intelligent design of multiple-section filters with economical damping of each section.

Consider the addition of a filter section to the input of an existing filter, as in Fig. 6. Let us assume that the existing filter has been correctly designed to meet the output impedance design criteria described in Section I: under the conditions $Z_a = 0$ and $v_g = 0$, $\| Z_o \|$ is sufficiently small. It is desired to add a damped filter section that does not significantly increase $\| Z_o \|$.

Middlebrook's extra element theorem [9] can be employed to express how addition of the filter section modifies Z_o:

$$\text{modified } Z_o = \left[Z_o\right]_{Z_a=0} \frac{\left(1+\frac{Z_a}{Z_N}\right)}{\left(1+\frac{Z_a}{Z_D}\right)} \tag{21}$$

where

$$Z_N = \left[Z_i\right]_{v=0} \tag{22}$$

is the impedance at the input port of the existing filter, with its output port shorted, and

$$Z_D = \left[Z_i\right]_{i=0} \tag{23}$$

is the impedance at the input port of the existing filter with its output port open-circuited. Hence, the additional filter section does not significantly alter Z_o provided that

$$\left\| Z_a \right\| << \left\| Z_N \right\| \tag{24}$$

and

$$\left\| Z_a \right\| << \left\| Z_D \right\| \tag{25}$$

Bode plots of the quantities Z_N and Z_D can be constructed either analytically or by computer, to obtain limits on Z_a. When $\| Z_a \|$ satisfies Eqs. (24) and (25), then the "correction factor" $(1 + Z_a/Z_N)/(1 + Z_a/Z_D)$ of Eq. (21) is approximately equal to 1, and the modified Z_o is approximately equal to the original Z_o.

A. Explicit Quantification of the Correction Factor

Additional insight into the effect of Z_a on Z_o can be obtained by plotting the magnitude of the $1/(1 + Z_a/Z_D)$ term, vs. the magnitude and phase of Z_a/Z_D. The result is illustrated in Fig. 7. This plot resembles the Nichols chart used in control theory; the equations are similar.

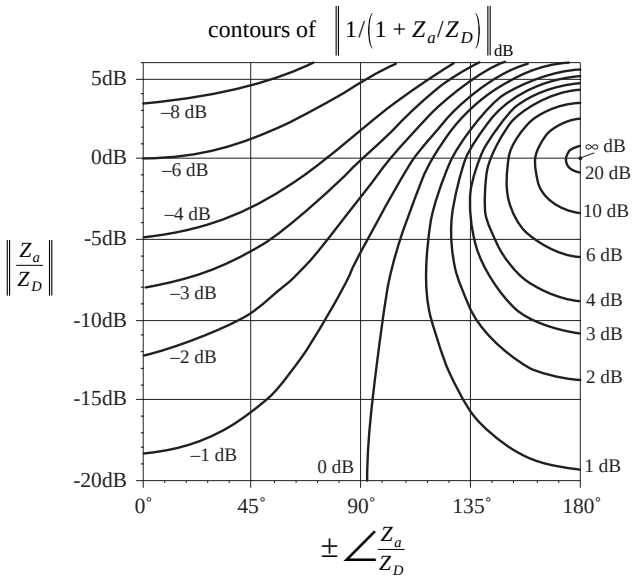

Fig. 7 Effect of the magnitude and phase of Z/Z_D on the magnitude of the correction factor term $1/(1 + Z/Z_D)$.

When Z_a is close in value to $-Z_D$, then the magnitude of $1/(1 + Z_a/Z_D)$ becomes large. Interaction between the existing filter and the added filter section then significantly increases the filter output impedance Z_o. One would expect a resonance to also appear in the filter transfer function.

To avoid increasing the magnitude of Z_o, the magnitude and phase of Z_a/Z_D must be chosen to lie to the left of the 0 dB contour of Fig. 7. In low-loss filters, it is usually not possible to accomplish this at all frequencies, because there are significant frequency ranges where Z_a is inductive and Z_D is capacitive, or vice-versa. The phase of Z_a/Z_D is therefore close to 180˚, and Fig. 7 predicts that $\| Z_o \|$ is increased. Nonetheless, the increase in magnitude can be minimal if $\| Z_a/Z_D \|$ is sufficiently small.

Since the poles of Z_o coincide with zeroes of Z_D, the minimum Z_D usually occurs at the peak of Z_o. Hence, it is advantageous to stagger-tune the filter. The frequency at which Z_a is maximum is chosen to be greater than the maximum frequency of Z_o, so that Eqs. (24) and (25) can be satisfied more easily.

The magnitude of the numerator term $(1 + Z_a/Z_N)$ can be plotted as a function of the magnitude and phase of Z_a/Z_N, in a manner similar to Fig. 7. The result is identical to Fig. 7, except that the dB magnitudes are inverted in polarity. When Z_a is close in value to $-Z_N$, then the magnitude of $(1 + Z_a/Z_N)$ becomes small. Interaction between the existing filter and the added filter section then leads to resonant zeroes in Z_o.

B. Example

As a simple example, let us consider the design of a two-section filter using R-L_d parallel damping in each section as illustrated in Fig. 8. It is required that the filter provide an attenuation of 80 dB at 250 kHz, with a peak filter output impedance that is no greater than approximately 3Ω.

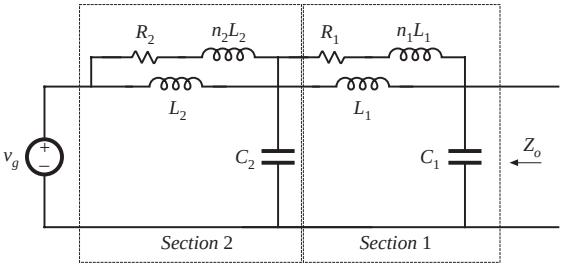

Fig. 8 Two-section input filter example, employing R-L_d parallel damping in each filter section.

As described in the previous subsection, it is advantageous to stagger-tune the filter sections so that interaction between filter sections is reduced. This suggests that the cutoff frequency of filter section 1 should be chosen to be smaller than the cutoff frequency of section 2. In consequence, the attenuation of section 1 will be greater than that of section 2. Let us (somewhat arbitrarily) design to obtain 45 dB of attenuation from section 1, and 35 dB of attenuation from section 2 (so the total is the specified 80 dB). Let us also select $n_1 = n_2 = n = L_d/L = 0.5$; as illustrated in Fig. 4, this choice leads to a good compromise between damping of filter resonance and degradation of high frequency filter attenuation.

Solution of Eq. (12) for the required section 1 characteristic impedance that leads to a peak output impedance of 3 Ω with $n = 0.5$ yields

$$R_0 = \frac{\| Z \|_{mm}}{\sqrt{2n\left(1+2n\right)}} = \frac{3\ \Omega}{\sqrt{2(0.5)\left(1+2(0.5)\right)}} = 2.12\ \Omega \tag{26}$$

Equation (13) and Fig. 4 predict that the R-L_d damping network will degrade the high frequency attenuation by a factor of $(1 + 1/n) = 3$, or 9.5 dB. Hence, the section 1 undamped resonant frequency f_1 should be chosen to yield 45 + 9.5 = 54.5 dB ⇒ 533 of attenuation at 250 kHz. Since

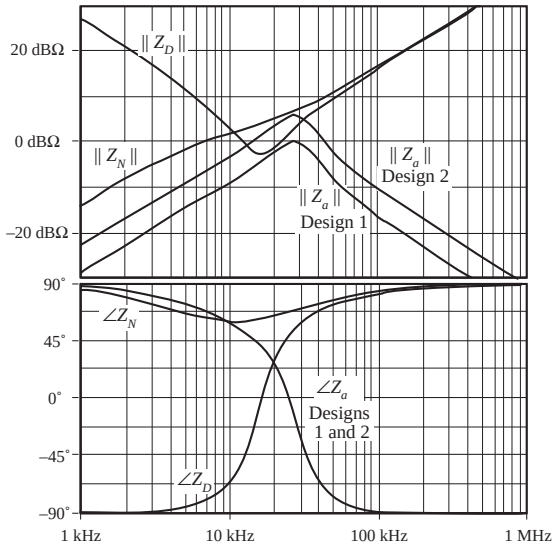

Fig. 9 Bode plot of Z_N and Z_D for filter section 1. Also shown are the Bode plots of Z_a for filter section 2 designs 1 and 2.

TABLE I
SECTION 2 DESIGNS

Parameter	Design 1	Design 2
R_0	0.71 Ω	1.41 Ω
max $\| Z_a \|$	1.0 Ω	2.0 Ω
f_0	19.25 kHz	19.25 kHz
f_m	27.22 kHz	27.22 kHz
n_2	0.5	0.5
L_2	5.8 μH	11.7 μH
C_2	11.7 μF	6.9 μF
$L_d = n_2L_2$	2.9 μH	5.8 μH
R_2	0.65 Ω	1.3 Ω

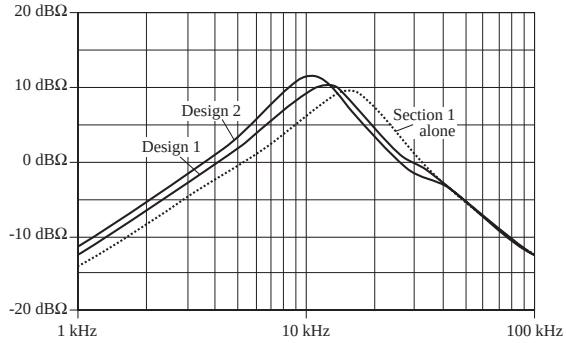

Fig. 10 Comparison of filter output impedance $\| Z_o \|$: section 1 alone, and cascade designs 1 and 2.

section 1 exhibits a two-pole roll off at high frequency, f_1 should be chosen as follows:

$$f_1 = (250\ \text{kHz}) / \sqrt{533} = 10.8\ \text{kHz} \tag{27}$$

The filter inductance and capacitance values are therefore

$$L_1 = \frac{R_0}{2\pi f_1} = 31.2\ \mu\text{H}$$
$$C_1 = \frac{1}{2\pi f_1 R_0} = 6.9\ \mu\text{F} \tag{28}$$

The section 1 damping network inductor is

$$n_1L_1 = 15.6\ \mu\text{H} \tag{29}$$

The section 1 damping resistance is found from Eq. (6):

$$R_1 = R_0Q_{opt} = R_0\sqrt{\frac{n\left(3+4n\right)\left(1+2n\right)}{2\left(1+4n\right)}} = 1.9\ \Omega \tag{30}$$

The quantities $\| Z_N \|$ and $\| Z_D \|$ for filter section 1 can now be constructed analytically or plotted via computer simulation.

Figure 9 contains plots of $\| Z_N \|$ and $\| Z_D \|$ for filter section 1, generated using SPICE. Also illustrated are the output impedances $\| Z_a \|$ for two choices (designated Design 1 and Design 2) of damped input filter section 2. To avoid significantly modifying the filter output impedance Z_o, the section 2 output impedance $\| Z_a \|$ must be sufficiently less that $\| Z_D \|$ and $\| Z_N \|$. It can be seen from Fig. 9 that this is most difficult to accomplish when the peak frequencies of sections 1 and 2 coincide. A better choice is to stagger-tune the filter sections, preferably by selecting the peak frequency of section to be greater than the peak frequency of section 1. Designs 1 and 2 both contain a section 2 undamped resonant frequency f_2 of 19.25 kHz, chosen in a manner similar to that used for Eq.

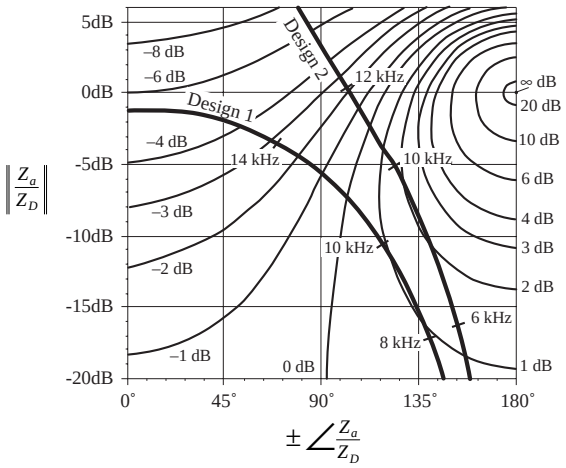

Fig. 11 Z_a/Z_D data overlaid on the plot of Fig. 7. Both design cases are illustrated.

(27). This leads to a peak frequency of 27.22 kHz, as given by Eq. (11). Thus, the section 1 and section 2 peak frequencies differ by a factor of almost 2.

Parameters for designs 1 and 2 are summarized in Table I. Values were computed in the same manner used for section 1 in Eqs. (26)-(30). The resulting output impedance $\| Z_o \|$ is plotted in Fig. 10. It can be seen that the filter output impedance is moderately increased at frequencies where $\| Z_a \|$ is comparable to $\| Z_N \|$ or $\| Z_D \|$.

Figures 11 and 12 illustrate the magnitudes of the numerator and denominator correction-factor terms. In Fig. 11, a SPICE listing of Z_a/Z_D data is plotted over the curves of Fig. 7. The denominator correction factor term leads to the greatest increase in $\| Z_o \|$ over the frequency range 5-11 kHz, because of the significant phase shift between Z_a and Z_D. Over the 12-32 kHz frequency range where $\| Z_a \| > \| Z_D \|$, the denominator correction factor term actually *decreases* the filter output impedance $\| Z_o \|$, because the phase shift between Z_a and Z_D is reduced. Figure 12 is a similar plot illustrating the effect of the numerator correction-factor term. This term leads to increased filter output impedance at frequencies where Z_a and Z_N have similar magnitudes and phases (approximately 8-25 kHz).

The complete filter function $\| H \|$ is plotted in Fig. 13. Both designs indeed meet the design goal of 80 dB of attenuation at 250 kHz. Thus, multiple damped filter sections can be cascaded to obtain an economical design. The approach used here yields insight into selection of filter section corner frequencies and characteristic impedances, such that interaction between stages is minimized.

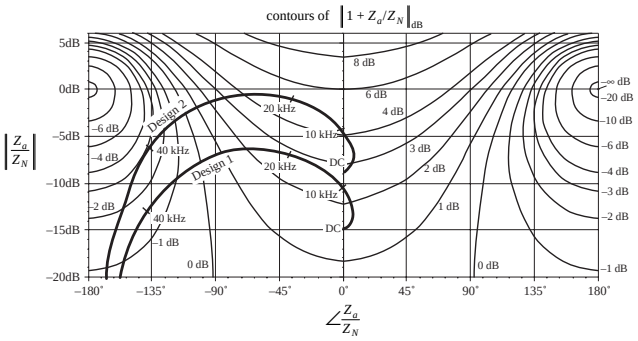

Fig. 12 Z_a/Z_N data, overlaid on contours of constant $\|1 + Z_a/Z_N\|_{dB}$.

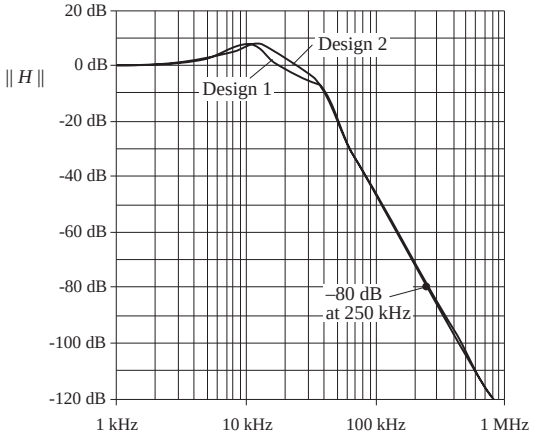

Fig. 13 Filter transfer function $\| H \|$, designs 1 and 2.

REFERENCES

[1] R. D. Middlebrook, "Input Filter Considerations in Design and Application of Switching Regulators," IEEE Industry Applications Society Annual Meeting, 1976 Record, pp. 366-382.

[2] R. D. Middlebrook, "Design Techniques for Preventing Input Filter Oscillations in Switched-Mode Regulators," Proceedings of Powercon 5, pp. A3.1 – A3.16, May 1978.

[3] T. K. Phelps and W. S. Tate, "Optimizing Passive Input Filter Design," Proceedings of Powercon 6, pp. G1.1-G1.10, May 1979.

[4] Y. Jang and R. W. Erickson, "Physical Origins of Input Filter Oscillations in Current Programmed Converters," *IEEE Transactions on Power Electronics*, vol 7, no. 4, pp. 725-733, October 1992. Also presented at APEC 91, paper can be downloaded from ece-www.colorado.edu/~pwrelect.

[5] S. Erich and W. M. Polivka, "Input Filter Design for Current-Programmed Regulators," IEEE Applied Power Electronics Conference, 1990 Proceedings, pp. 781-791, March 1990.

[6] N. O. Sokal, "System Oscillations Caused by Negative Input Resistance at the Power Input Port of a Switching Mode Regulator, Amplifier, Dc/Dc Converter, or Dc/Ac Inverter," IEEE Power Electronics Specialists Conference, 1973 Record, pp. 138-140.

[7] S. S. Kelkar and F. C. Lee, "A Novel Input Filter Compensation Scheme for Switching Regulators," IEEE Power Electronics Specialists Conference, 1982 Record, pp. 260-271.

[8] S. Singer and R.W. Erickson, "Power-Source Element and Its Properties," *IEE Proceedings — Circuits Devices and Systems*, vol. 141, no. 3, pp. 220-226, June 1994.

[9] R. D. Middlebrook, "Null Double Injection and the Extra Element Theorem," *IEEE Transactions on Education*, vol. 32, no. 3, pp. 167-180, August 1989.

[10] R. W. Erickson, *Fundamentals of Power Electronics*, New York: Chapman and Hall, pp. 697-705, 1997.